

# A Kalman Filter Approach Applied to the Qualitative Assessment of Structural Damage

Giovanni Facchin, Alfonso Nappi\*

Department of Engineering and Architecture, University of Trieste, Italy

\*Corresponding Author: [nappi@units.it](mailto:nappi@units.it)

Copyright © 2014 Horizon Research Publishing All rights reserved.

**Abstract** The paper is concentrated on a non-traditional application of the Kalman Filter algorithm and outlines a procedure that can be used to assess structural damage. The technique is essentially based on the estimate of unknown stiffness parameters of the structure, whose changes over time can be related to the structure's deterioration and local damage. In this way, suspected areas can be detected and further investigated. In our approach, it is assumed that experimental records are taken at regular intervals by means of shaking tests and/or during micro-seismic activity, so that optimal values of convenient parameters can be determined by solving an inverse problem. The proposed procedure has been applied to the estimate of bulk and shear modules, whose changes denote possible damage due to isotropic and deviatoric stress components, in accordance with the theoretical framework which several damage models are based on. More specifically, we simulated experimental tests on dam structures by assuming some damage at certain locations. Finally, an error indicator was introduced, with the aim of finding an objective measure of the accuracy of the results obtained by solving the inverse problem.

**Keywords** Dam Engineering, Damage Mechanics, Error Indicator, Finite Elements; Kalman Filter, Monitoring, Non-Destructive Tests, System Identification

---

## 1. Introduction

Structural safety and damage assessment are key elements in the field of structural engineering [1-6]. Here, we address the issue of monitoring and make use of a parameter estimation technique which appears to be suitable for detecting possible damage processes by exploiting experimental measurements (e.g., records taken during micro-seismic activity and/or artificial excitation tests).

Given a deterioration process, the actual damage depends on local defects (such as voids and/or cracks and/or material degradation). So, it is not surprising that an impressive amount of research work is centered on the detailed study of

specific phenomena—especially crack growth.

Alternatively, it is possible to focus on the average effect of damage on structural components and/or potentially critical parts of structural systems. Such average effect, in general, implies a loss of stiffness, which usually comes together with a loss of strength, as happens at the material level in the presence of softening.

In this work, we discuss a monitoring technique, which is suitable to detect the zones of a structural system that might be affected by damage. To this aim, we assume that critical areas are identified and modeled as macroscopically homogeneous zones characterized by linear elastic behavior. Next, we consider an input (e.g., excitation caused by vibrodynes or micro-seismic activity) and take records of displacements and/or velocities and/or accelerations. Finally, by solving an inverse problem, we estimate optimal values of a priori unknown parameters and check how they evolve over time.

In order to solve the inverse problem, we followed a Bayesian approach (in which both the measured data and the unknown parameters were non-deterministic quantities). As often done in different research fields [7-9], we made use of the Kalman Filter by working in the time-domain and considering the unknown parameters as state variables.

The proposed method was developed and tested with the aim of estimating bulk and shear modules, because these parameters play a central role in several material models that describe damage effects and take into account the action of both isotropic and deviatoric stress components [10-12].

Someone might remark that the information provided by elastic constants appears to be of limited interest. Yet, it should be noted that we intend to investigate structural systems subjected to typical (ordinary) load conditions, which mostly imply a response in the elastic range. In addition, possible changes of stiffness parameters are implicitly related to the nonlinear behavior of the material. In fact, a significant decrease of an average bulk modulus and/or shear modulus eventually captures and quantifies the influence of (local) nonlinear phenomena at a macroscopic level. Therefore, it appears that elastic properties, too, can efficiently denote the development of undesired nonlinear

effects and provide an indirect measure of different damage levels.

It can also be argued that vibration frequencies and vibration modes could be used as measured data, as proved by well documented case histories of civil engineering structures (e.g., bridges, historical buildings, skyscrapers, dams, just to name a few examples). However, we did prefer to focus on a different approach since we aim at determining (with a reasonable degree of accuracy) the zones, which are affected by damage (i.e., subjected to local deterioration, which, in turn, is reflected in a change of the mechanical properties of a macroscopically homogeneous material). Thus, the solution of an inverse problem in the time-domain is more suitable to achieve this goal, since local damage hardly affects eigenvalues and eigenvectors, which rather depend on the overall properties of structural systems.

So far, we have tested the proposed procedure by means of numerical simulations. Discrete models based on the finite element method were considered and fictitious experimental records were generated by computing the structural response to a given ground acceleration. Next, these records were used as measured quantities in order to estimate optimal values of stiffness parameters on the basis of a convenient a priori knowledge (initial values suggested by engineering judgment), as typical of Bayesian approaches.

We carried out some initial tests by using the same mesh to generate the fictitious measurements and estimate the parameters. In this way, it was possible to check the numerical procedure. In fact, we knew the actual values of the unknown parameters and we were sure that the algorithm (if properly implemented) had to converge to the correct solution. In other words, we began to estimate the parameters by following a procedure in which modeling errors did not play any role, because they simply did not exist. Therefore, the relevant results had to be accurate.

Next, we did consider modeling errors. Even though we continued to focus on numerical simulations, we made use of different discrete models: (i) a refined mesh to represent the actual structure and generate the fictitious experimental records, (ii) a coarse model to estimate the parameters. Consequently, our estimates were affected by modeling errors, as well as it necessarily happens in the case of in-situ tests.

In an effort to simulate real-life situations in the best possible way, we also took into account the fact that the actual values of the parameters and the most appropriate models are often unknown when a structure is investigated. Therefore, we introduced an error indicator that can be used to select the very model, which is most likely to give an adequate description of the structural behavior.

More precisely, we considered both a non-dimensional and a dimensional coefficient that represent objective measures of the difference between the experimental response at some points and the numerical response at the same points (i.e., the response computed by means of a discrete model characterized by the parameter values that were determined after exploiting the experimental

information and after solving the inverse problem).

Eventually, our numerical simulations did confirm that the most accurate models lead to the least value of those coefficients: the smaller the error indicator, the better the discrete model (and the estimate of the a priori unknown parameters).

The procedure is quite general. So, it can be applied to a large variety of structures and we simulated a monitoring program on large dams, which appear to be of high interest in the field of civil engineering [13-21]. More importantly, these structures typically require maintenance programs, non-destructive tests and periodic inspections for obvious reasons: huge cost in terms of money and human lives (not to talk of the impact on public opinion in case of collapse).

We mainly focused on the estimate of parameters in the presence of damage and modeling errors. As expected, it turned out that modeling errors do affect the precision of the estimates, which often happen to be quite rough. However, we always found a clear decrease of stiffness whenever we determined optimal values of the parameters by considering fictitious experimental data, which had been generated by assuming the presence of damage. Therefore, the proposed method seems to be suitable to detect critical areas or, at least, give useful information about the development of damage processes in some specific regions of a structural system.

## 2. The Algorithm

In this Section we will give a general overview of the Kalman Filter technique [22] and will outline the main features of the algorithm that allows us to estimate unknown parameters by dealing with these quantities as if they were state variables. The basic ingredients of the Kalman Filter are a state equation and output equation, which are usually written in the form [23]

$$\mathbf{x}_{k+1} = \mathbf{A} \mathbf{x}_k + \mathbf{B} \mathbf{m}, \mathbf{y}_k = \mathbf{f}(\mathbf{x}_k) + \mathbf{n} \quad (1a,b)$$

Here,  $\mathbf{A}$  and  $\mathbf{B}$  are constant matrices, while the vectors  $\mathbf{x}$  and  $\mathbf{y}$  represent state variables and measured values. Both are assumed to be non-deterministic. Thus, they are defined in terms of mean values and covariance matrices. The vectors  $\mathbf{m}$  and  $\mathbf{n}$  denote Gaussian white noise sequences. Finally, the vector-valued function  $\mathbf{f}(\mathbf{x})$  describes the way in which the measurements depend upon the state variables.

In short, eqn. (1a) defines the linear evolution of a state variable vector during any time interval  $\Delta t = t_{k+1} - t_k$ , whereas eqn. (1b) establishes a relationship between observations and state variables at the time  $t_k$ , since the indices  $k$  and  $k+1$  refer to the values attained by certain vectors at times  $t_k$  and  $t_{k+1}$ , respectively.

If the function  $\mathbf{f}(\mathbf{x}_k)$  is linear, we immediately find an optimal solution  $\mathbf{x}_{k|k}$  (i.e., an estimate of  $\mathbf{x}$  at time  $t_k$ , which is determined by exploiting the experimental information  $\mathbf{y}_k$ ). Alternatively, we can state that it is possible to update the vector  $\mathbf{x}_{k|k-1}$  (an estimate of  $\mathbf{x}$  based on the a priori knowledge at time  $t_{k-1}$ ) thanks to the experimental information  $\mathbf{y}_k$

available at time  $t_k$ .

For linear systems, such estimate is simply given by the equation

$$\mathbf{x}_{k/k} = \mathbf{x}_{k/k-1} + \mathbf{G}(\mathbf{x}_{k/k-1}) \{y_k - \mathbf{f}(\mathbf{x}_{k/k-1})\} \quad (2a)$$

where

$$\mathbf{G}(\mathbf{x}_{k/k-1}) = \mathbf{C} \mathbf{L}^T [\mathbf{L} \mathbf{C} \mathbf{L}^T + \mathbf{S}_{nn}]^{-1} \quad (2b)$$

$\mathbf{G}(\mathbf{x}_{k/k-1})$  represents the so-called *gain matrix*, which depends upon the covariance matrix of the measurement errors  $\mathbf{S}_{nn}$ , the covariance matrix of the parameters  $\mathbf{C}(\mathbf{x}_{k/k-1})$  and the sensitivity matrix  $\mathbf{L}(\mathbf{x}_{k/k-1})$ . This array contains the derivatives of the measured quantities taken with respect to the *state variables*. Thus, it quantifies how measurements depend upon possible changes of the parameter values. Needless to say, the matrix  $\mathbf{L}$  is constant and readily available when  $\mathbf{f}(\mathbf{x}_{k/k-1})$  is linear.

At each time step, the matrix  $\mathbf{C}$  is updated through the equation

$$\mathbf{C}_{k/k} = \mathbf{C}_{k/k-1} - \mathbf{G}(\mathbf{x}_{k/k}) \mathbf{L}(\mathbf{x}_{k/k}) \mathbf{C}_{k/k-1} \quad (3)$$

with  $\mathbf{L}=\mathbf{L}(\mathbf{x}_{k/k-1})$  and  $\mathbf{C}=\mathbf{C}(\mathbf{x}_{k/k-1})$ .

When  $k=1$  (at the beginning of the identification procedure), we need to assign initial values to the parameters  $\mathbf{P}_{k/k-1}$ , their covariance matrix  $\mathbf{C}_{k/k-1}$  and the covariance matrix  $\mathbf{S}_{nn}$ . As for  $\mathbf{S}_{nn}$ , it depends on the instrument accuracy. Since measurement errors can be assumed to be statistically independent, we considered a diagonal matrix  $\mathbf{S}_{nn}=\text{diag}[(\sigma_m)^2]$ , where  $\sigma_m$  is the standard deviation of the  $m$ -th measured quantity ( $m=1, \dots, M$ , if  $M$  is the total number of observations).

Initial parameters, instead, are defined on the basis of previous practice and experience. If we have confidence in our assumption, it is possible to quantify such confidence by giving relatively small values to the elements of the covariance matrix  $\mathbf{C}$  (low variances obviously imply that the initial estimates are quite reliable). If we do so, the algorithm will slightly change the parameter values during the identification process.

Conversely, we can acknowledge poor confidence in our a priori estimates and assign relatively large values to the entries of  $\mathbf{C}$ . Consequently, the algorithm will try to adjust the parameter values with the aim of minimizing the difference between the numerical response and the experimental data. When we operate in this way, the final estimates will hardly depend on our initial guess.

As a rule of thumb, large values of the entries of  $\mathbf{C}$  should be considered when we investigate a structure with the aim of detecting possible damage in an area whose mechanical properties and boundaries are not clearly defined. Therefore, in view of the particular nature of our objective, we always assumed high initial variances in our numerical examples.

In the specific case of the problem we are dealing with, the vector  $\mathbf{x}$  coincides with the parameter vector, as anticipated at the beginning of this Section, when we pointed out that the *a priori* unknown parameters would play the role of state variables. In addition, these parameters are constant over

time (since we refer to bulk and shear modules, which are not time dependent). Thus, eqn. (1a) becomes

$$\mathbf{x}_{k+1} = \mathbf{x}_k \quad (4)$$

So, while the state equation is extremely simple, the function  $\mathbf{f}(\mathbf{x})$  in the output equation is nonlinear. This fact involves a considerable computational burden (as typical of the so-called *Extended Kalman Filter*). In fact, an iterative procedure should be applied at each time step. More precisely, we should make use of a recursive formula at each time step, instead of updating the state variables by means of eqn. (2a). In other words, the optimal values of the parameters should be determined by means of the equation

$$\mathbf{x}_i = \mathbf{x}_{i-1} + \mathbf{G}(\mathbf{x}_{i-1}) \{y_k - \mathbf{f}(\mathbf{x}_{i-1})\} \quad (5)$$

where the index  $i$  denotes the  $i$ -th iteration and  $\mathbf{x}_{i-1}$  represents  $\mathbf{x}_{k/k-1}$  for  $i=1$ . Of course, the iterative process would come to an end when a convenient norm of  $\{\mathbf{x}_i - \mathbf{x}_{i-1}\}$  is below a given tolerance. The obvious risk is that a large number of iterations are needed at each step before converging to the final estimate.

As discussed in Section 4, it is possible to obtain correct estimates of the unknown parameters by drastically reducing the computational effort. Indeed, we can simply apply eqn. (2a) as if the process were linear. This means that we need to set  $\mathbf{L}=[\partial\mathbf{f}/\partial\mathbf{x}]$ , compute the derivatives for  $\mathbf{x}=\mathbf{x}_{k/k-1}$  and proceed to the following time step after determining  $\mathbf{x}_{k/k}$  through eqn. (2a). When all the time steps have been considered (*i.e.*, when we have exploited all the information given by an experimental record and have found the last estimates of the parameters), we start it all over again by using the same experimental record and assuming the last values of the unknown parameters as initial guess for a new identification process. As we would do in the case of the iterative procedure, we stop the process when a convenient norm of  $\{\mathbf{x}_L - \mathbf{x}_p\}$  is below a given tolerance, where  $\mathbf{x}_L$  is the final estimate at the end of the last identification process, while  $\mathbf{x}_p$  is the final estimate at the end of the previous process.

### 3. An Error Indicator

In view of their intrinsic features, numerical simulations are performed in a context in which the correct solutions are known. In consequence, it is easily possible to check the accuracy of the final estimates. Instead, the context in which we perform in-situ tests is quite different: in principle, any estimate might be wrong or reasonably accurate (provided that it is consistent with the basic properties of the structure under investigation). Therefore, it is of practical interest to establish a criterion that allows us to choose among different discrete models (which may differ from one another in terms of degrees of freedom and/or locations of the suspected areas and/or other details).

In order to assess the quality of the estimates, it is possible to define a convenient error indicator (*i.e.*, an

unbiased index of the accuracy of the estimates). Such an index can be determined by considering  $N$  measured quantities (displacements and/or velocities and/or accelerations at some points) at  $T$  time-steps during a time-interval, in which the structure was subjected to an external excitation. Next, after estimating the parameters on the basis of a certain discrete model, we can use the same model, introduce the estimated parameters and compute the response to the external excitation that occurred when we took the  $N$  measurements. At this stage, we only need to compare the numerical and experimental responses at each time-step by defining the non-dimensional coefficient

$$\xi = \left\{ \sum_{i=1,N} \sum_{j=1,T} [(Q_{ij} - M_{ij})^2 / (M_{ij})^2] \right\}^{1/2} \quad (6)$$

where  $Q_{ij}$  represents a computed quantity and  $M_{ij}$  the corresponding measured quantity.

The coefficient  $\xi$  is related to the reliability of the estimates, since it takes into account the overall structural response, which depends upon the discrete model, the mechanical properties and the correct (or incorrect) selection of the critical zones. In other words, the index  $\xi$  essentially reflects the accuracy of the mesh that has been used to estimate the unknown parameters.

In what follows, we will briefly discuss the role of the error indicator  $\xi$ . To this aim, we will report some results of a previous work [24]. On that occasion, we considered the Pian Telesio Dam, in North-West Italy, by assuming some through-the-thickness damage in a portion of the structure. For the numerical analysis, we made use of 20-node isoparametric elements, arranged along a certain number of layers. The external surface of the zone that was assumed to be damaged is schematically shown in Fig. 1 (Z1, downstream of the dam). This zone, delimited by thick lines in Fig. 1, was discretized by means of four elements per layer. Point P denotes the position of the surface node, which is in common with the elements of the external layer.

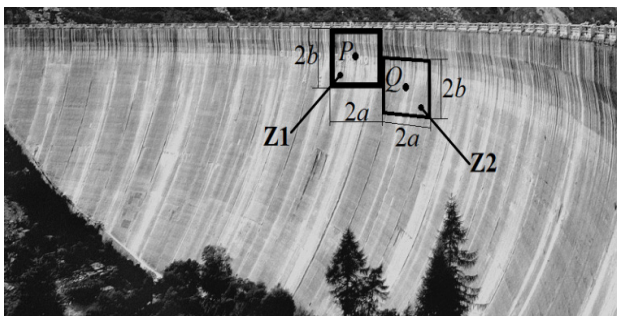


Figure 1. View of the Dam that was Considered in Order to Test the Effect of Modeling Errors on the Error Indicator  $\xi$

By using a five-layer mesh, we generated fictitious experimental measurements. Next, the virtual measured response was exploited to estimate the unknown parameters. In this phase, we made use of different discrete models (all consisting of three layers in order to introduce a first source of modeling errors).

We considered different (hypothetically damaged) portions of the dam, where the stiffness properties were to be estimated. We started by computing optimal values of the a priori unknown parameters in the same region that was assumed to be damaged. Therefore, point P in Fig. 1 was again the surface node, which was in common with the four elements of the external layer. Instead, in the subsequent numerical tests, we introduced another modeling error. In fact, we estimated the elastic constants in regions (of similar dimensions) which were shifted to the right or to the left and/or downward. Again, these regions were discretized by using four elements per layer. However, the common node on the external surface was displaced (approximately, a or 2a to the right or to the left and/or b or 2b downward). For instance, point Q (inside zone Z2 in Fig. 1) is at distance 2a to the right and at distance b downward with respect to P.

In this way, we made use of fifteen discrete models, each time considering a different portion of the dam, which was assumed to be affected by damage. Instead, the zone, which was actually damaged and was utilized to generate the fictitious measurements, was always the same. In the end, we estimated fifteen sets of a priori unknown parameters.

As expected, we obtained different results. Then, for each set of estimated parameters, we computed the numerical response of the structure to a given input. To this purpose, we used the same ground acceleration and the same numerical model (three-layer mesh) that had allowed us to find the unknown elastic constants by means of the Kalman Filter.

More specifically, we determined the accelerations at ten points and found out the values of  $\xi$ , as given by eqn. (6). The relevant results are summarized in Fig. 2. The front surface shows to the trend of the non-dimensional coefficient  $\xi$  when we estimated the elastic constants in zone Z1 and in regions to the left or to the right with respect to Z1. The second surface refers to the estimates of the stiffness parameters in Z2 and in the other regions aligned with Z2, while the third surface is concerned with the estimates in the five bottom zones. Note that the black dots in Fig. 2 correspond to the values of  $\xi$ , which were computed by considering the estimates in the zones Z1 and Z2.

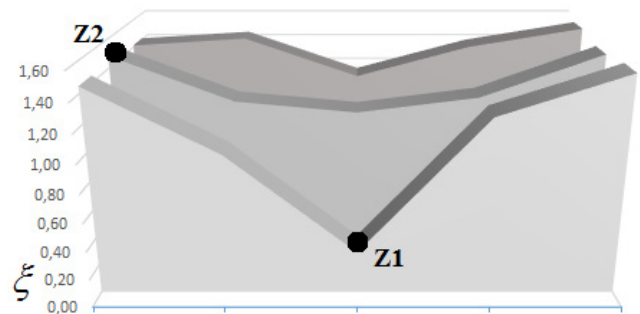


Figure 2. Relationship between the Non-Dimensional Coefficient  $\xi$  and Modeling Errors

Clearly,  $\xi$  tends to increase when the unknown parameters are estimated in regions, which do not coincide with Z1 (the

zone, which is affected by some damage).

For obvious reasons, any term  $M_{ij}=0$  must be excluded from the summation (together with the companion term  $Q_{ij}$ ). Actually, in our numerical simulations we did not include any term  $M_{ij}$  whose absolute value was less than  $10^{-3}M_{MAX}$ , where  $M_{MAX}$  was the largest absolute value of the corresponding measured quantity (displacement and/or velocity and/or acceleration). In fact, when a measured quantity approaches zero, there might be numerical errors that improperly lead to exceedingly high values of  $\xi$ . For instance, if  $M_{MAX}=10$  units and  $M_{ij}=10^{-6}$  units, a computed quantity  $Q_{ij}=10^{-8}$  units would imply a negligible computational error, but it would cause the index  $\xi$  to dramatically increase.

It is obvious, however, that any threshold is absolutely arbitrary and that the value of  $\xi$ , as defined in eqn. (6), can be badly affected by numerical errors, even when they are of minor importance.

Therefore, in this work we preferred to consider the dimensional coefficient

$$\xi^* = \sum_{i=1,N} \sum_{j=1,T} |Q_{ij} - M_{ij}| \Delta t_j \quad (7)$$

where  $|\bullet|$  denotes the absolute value of  $\bullet$ , while  $\Delta t_j$  represents the time interval during which  $Q_{ij}$  and  $M_{ij}$  can be assumed as average values of the computed and measured quantities. Therefore, eqn. (7) essentially approximates the sum of the  $N$  integrals

$$\int |Q_i(t) - M_i(t)| \quad (8)$$

computed between 0 and  $T_R$ , if  $T_R$  denotes the record length. In the above integral, the index  $i$  clearly refers to the  $i$ -th record or the computed/measured quantity at the  $i$ -th point.

#### 4. Preliminary Tests to Investigate the Reliability of the Proposed Procedure

Before assuming any structural damage and before investigating the capability of the proposed approach to detect ongoing deterioration processes, numerical tests were performed with the aim of determining some basic features of the parameter estimation technique, taking into account the specific context to which the Kalman filtering approach had to be applied.

At the very beginning, we focused on the sensitivity of the measured quantities with respect to possible changes of the mechanical properties. To this purpose, the dam-basin model of the previous Section was considered and the three-layer mesh was used to generate fictitious experimental records. First, we computed the structural response to a given input signal by assuming a macroscopically homogeneous material characterized by a uniform distribution of elastic properties across the entire dam (Young's modulus  $E=28,800$  MPa and Poisson's ratio  $\nu=0.2$  or, alternatively, bulk modulus  $K=16,000$  MPa and shear modulus  $G=12,000$  MPa).

Next, we selected four zones, each consisting of three layers and six 20-node isoparametric elements per layer. These particular regions of the structural system are shown in Fig. 3, where the shaded areas represent the external surfaces of each zone. By changing the elastic constants ( $\pm 10\%$ ) of the four zones, we could check the effect on the measurable quantities at some points. As expected, we found out that the numerical results highly depended on the values of  $E$  and  $G$ , while the bulk modulus  $K$  had a smaller effect on the measurable quantities. As for Poisson's ratio, the consequences of any changes appeared to be practically negligible.

Our mesh was based on a numerical model developed in the framework of an ICOLD benchmark study [25]. Such model was concerned with an arch-gravity dam (*cf.* Fig. 1) and the relevant reservoir at Pian Telesio, Italy. The reservoir total capacity was over  $23 \cdot 10^6$  m<sup>3</sup>, while the maximum height of the structure was 80 m and the crest length 515 m. In order to properly apply the loads induced by the ground motion, we considered the surrounding bedrock, in accordance with the model for the ICOLD benchmark. Eventually, the discrete model of the dam-foundation system was about 500 m deep and included a fairly large portion of the bedrock, which was approximately circular in cross section, with a diameter around 1,500 m.

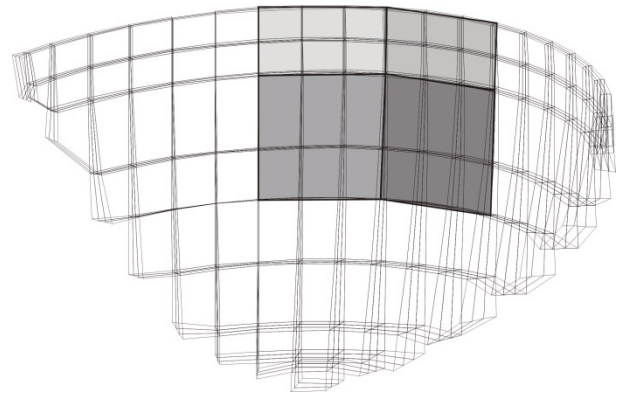


**Figure 3.** Four Zones of the Structural System that were Selected in Order to Check How Measurable Quantities Depend Upon Local Changes of the Mechanical Properties

Since the aim of the present work was to check a testing procedure that should be able to detect possible deterioration processes in macroscopically homogeneous zones, we assumed that joints (a main source of nonlinear effects) played a marginal role. Therefore, a linear elastic behavior was considered for the whole structure.

The experimental records were generated by subdividing the load history into a certain number of time steps (120 in this specific case) and by computing the incremental response during each step by means of an explicit algorithm. Next, the estimate process was carried out in a similar way, since  $\mathbf{f}(\mathbf{x}_{k|k-1})$  in eqn. (2a) and  $\mathbf{f}(\mathbf{x}_{i-1})$  in eqn. (5) represent the response of a system at time  $t_k$  on the basis of the information available at time  $t_{k-1}$ . Therefore, if the system is

linear or assumed to be linear, the incremental solution is immediately available by considering a stiffness matrix, which is constant during the time step and depends upon the parameter values at the beginning of that step. Conversely, when we apply eqn. (5), the incremental solution is computed by considering a stiffness matrix, which is constant during the time step and eventually depends upon the parameter values at the end of that step.

Our preliminary results (aimed at checking the properties of the sensitivity matrix  $L$ ) are summarized in Figs. 4 and 5. The plots show how the acceleration at a point changes when the elastic properties are subjected to a  $\pm 10\%$  increment in four different zones of the structure. The curves that denote the most evident changes are due to different values of  $E$  and  $G$ , respectively. Instead, the changes of the structural response tend to be smaller (Fig. 5) when  $K$  is increased or decreased. As for Poisson's ratio, different values of  $\nu$  cause minor effects (as shown by the curve that oscillates around the horizontal axis in Fig. 4).

On the basis of these tests, it was pretty evident that there was no point in trying to estimate Poisson's ratios. We could either focus on a single parameter (the elastic modulus) or consider  $G$  and  $K$  (most likely, with better accuracy in the case of the shear modulus). Instead, had we chosen Young's modulus and Poisson's ratios as unknown parameters, it would have been impossible to properly estimate Poisson's ratios.

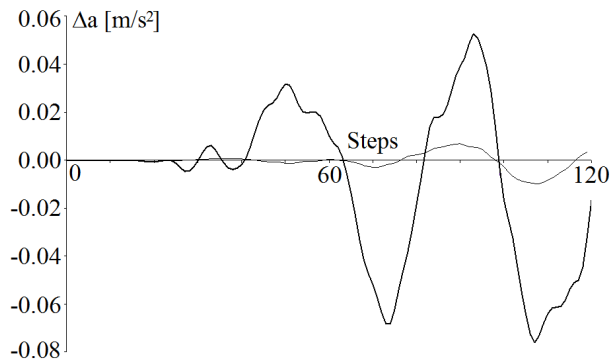


Figure 4. Sensitivity Test on Young's Modulus and Poisson's Ratio

As already pointed out, several damage models focus on deviatoric stresses as well as isotropic stresses, since both components usually affect damage processes through different mechanisms. Therefore, we decided to implement the Kalman Filter in the framework of a numerical procedure that would be able to detect possible changes of  $G$  and  $K$  in existing structures.

After selecting the parameters to be estimated, we tried to optimize the algorithm, since the computational burden was quite relevant because of two main reasons. First, every time we update a parameter vector by means of the Kalman Filter equations, we need to define a new gain matrix and, hence, it is necessary to find a new sensitivity matrix  $L$ , which consists of the derivatives of the measured quantities (displacements and/or velocities and/or accelerations) with respect to the unknown parameters. Unfortunately, such

derivatives can only be computed numerically.

In consequence, for each parameter, it is required that we slightly change its value, compute the structural response and determine the ratios between the increments of the measured quantities and the increment of the parameter. This means that the stiffness matrix needs to be computed over and over again. However, in practical problems, only a few entries of the stiffness matrix depend upon the current values of the unknown parameters. Clearly, these entries are concerned with the finite elements that belong to the regions where damage processes might occur and a priori unknown parameters are to be estimated.

Therefore, we applied the substructuring technique. In this way, we could update the global stiffness matrix by means of simple algebraic operations that essentially involved a relatively large constant matrix (the one concerned with given elastic properties) and relatively small matrices that we continually needed to update by considering the current values of the parameter vector.

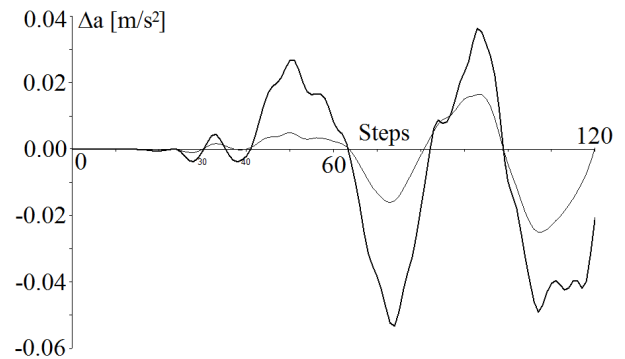


Figure 5. Sensitivity Test on Shear and Bulk Modules

A second problem, already mentioned, had to do with the nonlinear relationship between the measurable quantities and the unknown parameters. In view of this relationship, we should activate an iterative procedure at each time step and use eqn. (5). For instance, this is the case of the results plotted in Fig. 6.

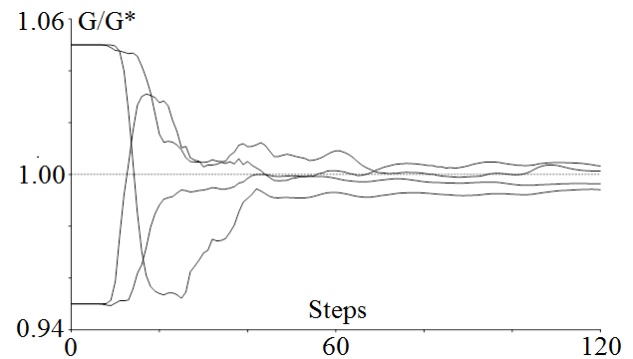


Figure 6. Estimate of Four Shear Modules by Using Eqn. (5)

Fig. 6 shows the details of an estimate of the shear modulus (with  $G^*$  denoting the correct value). The identification process was carried out by assuming that both the bulk and shear modulus were unknown in the zones

clearly marked in Fig. 3.

We made use of eqn. (5) and obtained excellent results, since modeling errors did not affect the system identification process. In fact, the same three-layer mesh was used to discretize the structural system (when the fictitious measurements were generated) and to estimate the unknown parameters.

Note that the fictitious experimental records were determined by assuming that there was no damage in the four zones ( $G = G^* = 12,000$  MPa and  $K = 16,000$  MPa).

However, as already discussed in a previous paper [26], accurate results can also be obtained if we consider a certain experimental record, assign reasonable initial values to the unknown parameters and estimate the elastic constants as if the system were linear.

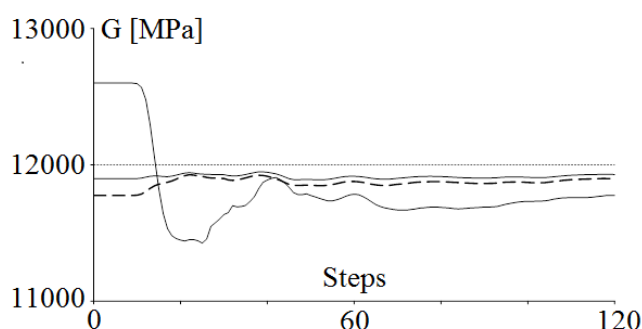


**Figure 7.** Estimate of the Shear Modulus in the Top Left Zone of Fig. 3 by Assuming that the System Is Linear And By Repeating the Identification Process Until Convergence (Thin Solid Curve: First Estimate – Thick Solid Curve: Final Estimate)

Of course, there is a cost to be paid, because the identification process must be repeated a few times, until a convenient measure of the difference between two sets of estimated values does not exceed a given tolerance. In other words, we can use eqn. (2a) and update the sensitivity matrix  $L = [\partial f / \partial x]$  just once at each time step (by setting  $x = x_{k/k-1}$ ). Then, after considering the whole experimental record, we need to start it all over again, by assuming the final values of the previous estimation process as initial values for the new process.

As shown in Fig. 7, which refers to a bulk modulus, the procedure continues until a convenient norm of the difference between two subsequent estimates is negligible. The results in Fig. 7, too, were obtained without including modeling errors and are similar to the results given by eqn. (5).

Therefore, the parameters can be properly estimated by dealing with the system as if it were linear. This implies a big saving in CPU time, since the identification process must be usually repeated a few times, while many more iterations are often required at each time-step when we

apply eqn. (5).

## 5. Simulated Monitoring Activity

As obvious, the estimates cannot be so accurate, when modeling errors are included with the aim of simulating real test conditions. Nonetheless, it did turn out that the proposed approach has the capability to provide useful information in the framework of possible monitoring activities. Indeed, even though it usually happened that the final estimates of the unknown parameters were not correct (not so good as in the numerical examples of Section 4), there was clear evidence that our algorithm was able to detect macroscopic areas where damage processes might have affected the structural integrity. It also appeared that the error indicator discussed in a previous Section could be a helpful tool to select the optimal model.

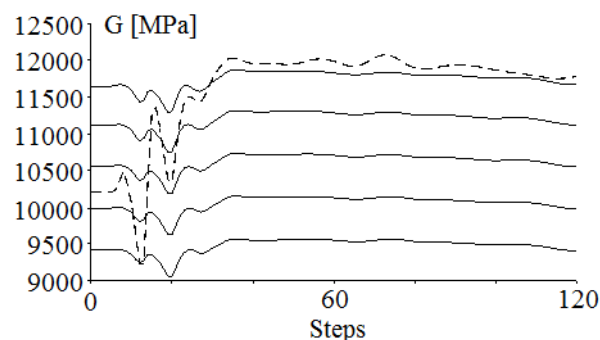


**Figure 8.** Estimate of the Shear Modulus in the Top Right Zone Of Fig. 3

Here, we will discuss a few cases, which seem to be of practical interest. The first example is concerned with the mesh in Fig. 3. We assumed some damage in the top right portion and generated fictitious measurements (accelerations and velocities) at thirty locations by means of the five-layer discrete model. In order to simulate different damage levels, we simply multiplied the initial shear and bulk modules (12,000 MPa and 16,000 MPa, respectively) by 0.95, 0.90, 0.85, 0.80. Next, we estimated the unknown parameters in the four zones with the three-layer model. Some results are shown in Figs. 8 and 9.

Namely, the plots refer to (i) the initial estimates of the shear modules in the top right portion and the bottom left portion (dashed curves) when no damage is present, when arbitrary initial values are assumed and when the unknown parameters are updated through eqn. (2a), as if the process were linear; (ii) the final estimates when the damage in the top right portion ranges between 0 and 20 percent (solid curves), so that the exact values in this sub-region should be 12,000, 11,600, 10,800, 10,200, 9,600 MPa, while the exact value in the bottom left zone should always be 12,000 MPa.

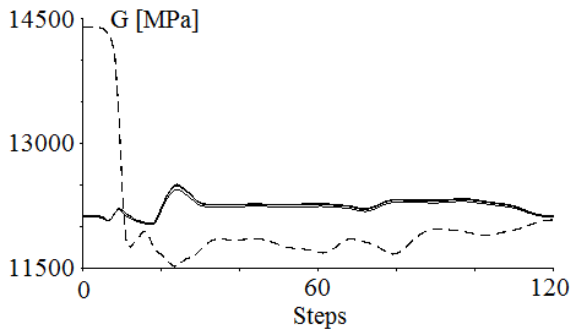


**Figure 9.** Estimate of the Shear Modulus in the Bottom Left Zone of Fig. 3

As explained in Section 2, the final estimates refer to the values obtained by repeating the computations (as if the process were linear) until the difference between the last two estimates does not exceed a certain tolerance, each time assuming the previous results as initial values for the new identification procedure. In our tests, we actually stopped the recursive algorithm when  $\|xL - xP\|/\|xP\|$  was less than  $10^{-2}$ , where  $\|\bullet\|$  denotes the Euclidean norm of  $\bullet$ .

Similar results were obtained by considering a different configuration: four zones, all aligned on top of the dam, where the stiffness parameters were assumed to be *a priori* unknown. Again, fictitious measures were determined on the basis of a five-layer mesh by imposing different damage levels in a single zone, while the parameters were estimated by means of a three-layer mesh. Some results, concerned with the bulk modulus, are shown in Figs. 10 and 11.

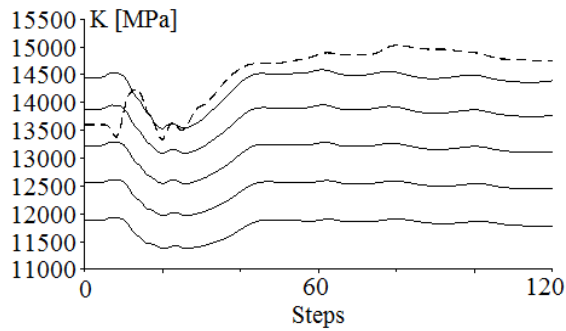


**Figure 10.** Estimate of the Bulk Modulus in the Damaged Zone When the Elastic Constants are Estimated in Four Zones (Three Of Which Are Assumed to be Undamaged)

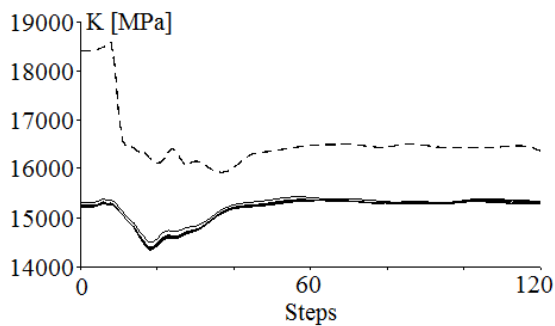


**Figure 11.** Estimate of the Bulk Modulus in an Undamaged Zone when the Elastic Constants are Estimated in Four Zones (One of Which is Assumed to be Damaged)

This time the estimates are less accurate, but the discrepancies are fully consistent with the fact that bulk modules are less sensitive to parameter changes, as pointed out in Section 4 and, more specifically, as shown by the plots of Fig. 5.

Even though the errors are not negligible, the numerical approach discussed here and based on the Kalman Filter (i.e., on an algorithm that works in the time domain) does provide useful information about the ongoing damage processes. In fact, the estimated values are approximately the same in the undamaged zone, while the stiffness parameters definitely decrease in the zone, which is affected by damage.

We can also observe that a nearly constant change of the parameter estimates occurred each time we imposed a 5% change to the elastic constants that were introduced into the five-layer mathematical model and were utilized in order to generate the fictitious measurements.

So far, the modeling errors have only been concerned with the discrete model, since we used a reasonably fine mesh to generate the fictitious recorded data and a coarse mesh to estimate the unknown parameters. Instead, the location and geometry of the damaged zones were assumed to be known.

In a further attempt to investigate the potential capabilities of the technique proposed in this paper, we also assumed to have a rough idea of the areas that might be affected by damage.

The fictitious experimental data, as usual, were determined by using a five-layer mesh and by considering a 10% damage in the top right zone (the one whose external surface was the quadrangle EFML in Fig. 12). Next, we introduced a 10% damage in the zone whose external surface was the quadrangle ACJG and, finally, a 10% damage in the zone whose external surface was the quadrangle BDKH.

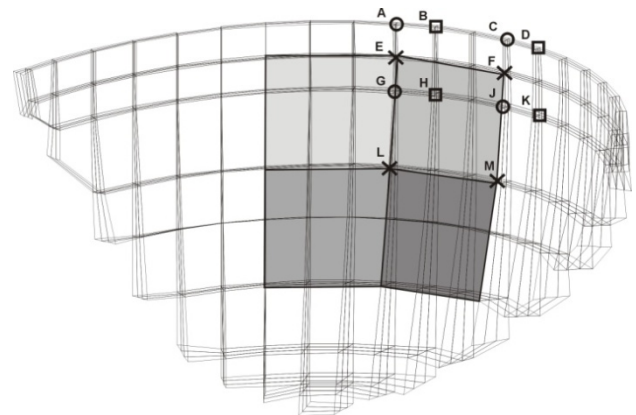


**Figure 12.** A Set of Four Zones Where a Priori Unknown Parameters were Assumed Shaded Areas and Vertices of the Quadrangles that Identify Three Different Zones Affected by Damage (ACJG, BDKH, EFML)

Fig. 13 shows a plane scheme, where the four zones in which we estimated the unknown parameters are marked in grey. In the same picture, we also see the regions affected by a 10% damage: zone 2 and zones delimited by thick



lines (solid and dashed lines). Finally, the dots within circles denote the points where fictitious measurements (generated by means of the five-layer model) were considered.

In view of the different meshes (one to generate fictitious measurements, one to estimate unknown parameters) and in view of the different zones where we tried to find optimal values of the elastic constants, we introduced significant modeling errors.

Clearly, the worst situation occurred when damage had to do with the zones delimited by thick lines in Fig. 13. Some results in terms of parameter estimates are shown in Figs. 14-16: (i) the bulk and shear modules in zone #2 of Fig. 13 when damage is assumed to be in the same zone; (ii) the shear modules in zone #1 of Fig. 13 when damage is assumed to be in the zone delimited by a dashed line.

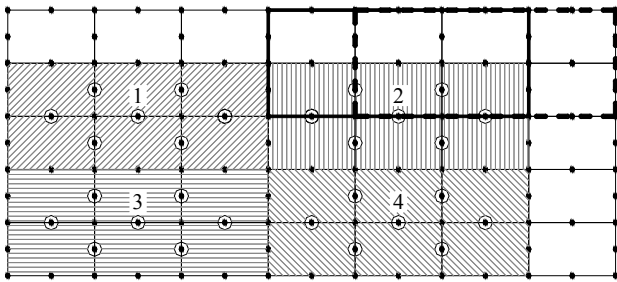


**Figure 13.** Plane Scheme that Shows The Zones (1-4) where Unknown Parameters were Assumed and the Zones where Damage was Introduced (Zone 2 and Zones Delimited by a Thick Solid or Dashed Line)

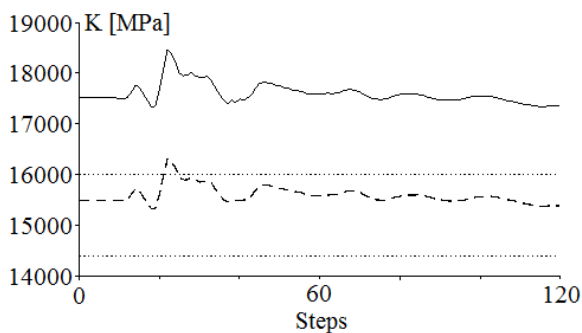


**Figure 14.** Estimate of the Bulk Modulus in Zone #2 of Fig. 13 when the Structure is Undamaged (Solid Curve) and when a 10% Damage is assumed in the Same Zone (Dashed Curve)

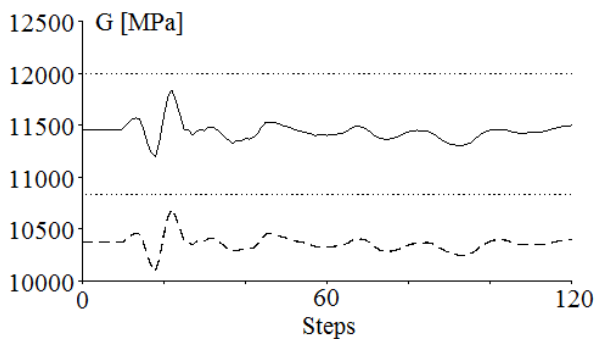


**Figure 15.** Estimate of the Shear Modulus in Zone #2 of Fig. 13 when the Structure is Undamaged (Solid Curve) and when a 10% Damage is Assumed in the Same Zone (Dashed Curve)

The solid curves in Figs. 14-16 refer to the estimates when there is no damage (so that the correct values should be  $K=16,000$  MPa and  $G=12,000$  MPa). The dashed curves, instead, are concerned with the damaged structure (note that  $K=14,400$  MPa and  $G=10,800$  MPa are the correct elastic constants in the zones where a 10% damage was assumed). The expected values of the parameters concerned with the undamaged structure and the damaged zones are shown with dotted lines in the figures.

Fig. 16 refers to a typical case in which the estimates are far from being accurate even when the structure is not damaged (owing to the modeling errors). However, the comparison between the solid and dashed curves do show that the mechanical properties of the structure have dramatically changed owing to some damage.

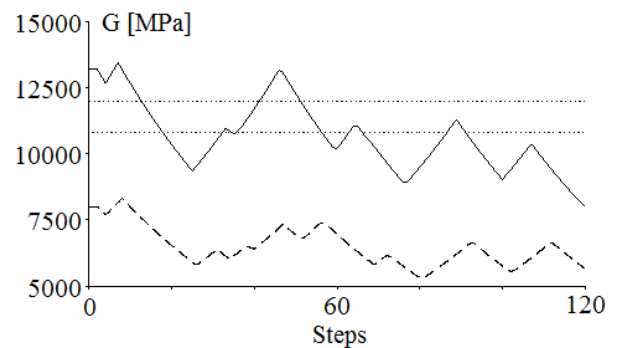


**Figure 16.** Estimate of the Shear Modulus In Zone #1 of Fig. 13 when the Structure is Undamaged (Solid Curve) and when a 10% Damage (Dashed Curve) is Assumed in the Zone Delimited by a Dashed Line in Fig. 13

We also checked the *error indicator*, computed on the basis of eqn. (7). We found its value by comparing the measured velocities and accelerations with the velocities and accelerations that were determined by using the three-layer model with the stiffness parameters estimated by means of the Kalman Filter approach. The index  $\xi^*$  was computed by considering thirty points along the top of the dam surface.

We obtained the following results:

- 0.15219 m and 2.54294 m/s, when damage was assumed to be in the zone delimited by a dashed line in Fig. 13
- 0.14753 m and 1.16912 m/s, when damage was assumed to be in the zone delimited by a thick solid line in Fig. 13
- 0.13188 m and 1.03014 m/s, when damage was assumed to be in the zone #2 of Fig. 13

These results actually confirm that the error indicator defined in eqn. (7) can effectively be used as an objective measure of the accuracy of the mathematical model. In fact, we obtained the lowest value of  $\xi^*$  when we considered the best mesh (i.e., the mesh that was used to estimate stiffness parameters in the region where the structure was actually damaged).

Finally, it is worth noting that the index  $\xi^*$  should be

evaluated by comparing measured and computed quantities at points that have nothing to do with the points where measurements are taken in order to estimate the unknown parameters.

In fact, the parameter estimation process leads to parameter values that make the measured and computed response as close as possible. Therefore, it may well happen that experimental records and numerical results at the measurement points are quite similar, even when severe modeling errors are included.

Instead, if we use the estimated parameters in order to determine the structural response at any point (preferably extraneous to the parameter identification procedure) it is likely that the best results are obtained when the most accurate model is considered.

For instance, we also tried to compute the index  $\xi^*$  by comparing the measured and computed response at the same points (dots within circles in Fig. 13) where fictitious measurements had been assumed to implement the system identification procedure. In this case, as expected, there were no significant differences between the values of  $\xi^*$ , which were determined by considering the three different sets of estimated parameters.

## 6. Closing Remarks

The paper has focused on a diagnostic method, which can be used to assess the conditions of existing structures through the estimate of elastic constants that are related to the strength and stiffness of macroscopically homogeneous zones, which are affected by possible damage processes.

The proposed approach is based on the Kalman Filter, a recursive filter that allows one to estimate the internal state of a linear dynamic system and is suitable for a large number of optimization problems, ranging from GPS navigation [27, 28] to hydrodynamics [29], from transportation engineering [30] to medicine [31].

Thanks to the Kalman Filter, we could determine the optimal values of unknown parameters by means of a dynamic analysis in the time domain. As already pointed out, we made this choice, since we were interested in local mechanical properties (while eigenvalues and eigenvectors tend to be sensitive to the overall features of structural systems).

So far, we have only focused on numerical simulations. Thus, we generated fictitious experimental records, by computing the response of a certain system (a dam) to a given input signal (a ground acceleration, assumed to be caused by micro-seismic activity). Alternatively, depending on the structure of interest, vibrations can be artificially induced by means of vibrodynes.

Whatever the input, displacements and/or velocities and/or accelerations at some points can be considered as measured quantities, which allow us to solve an inverse problem. In this way, we eventually estimate optimal values of stiffness parameters starting from a convenient a priori

knowledge (e.g., initial values suggested by engineering judgment).

Simulated tests gave us the opportunity to evaluate the potential effectiveness of the method, since it was possible to create testing conditions in which the correct results were available (because no modeling errors were included). Therefore, we could check the effectiveness of the system identification algorithm and verify that the Kalman Filter approach was actually able to provide accurate results.

By properly changing the testing conditions, we included modeling errors at different levels. The easiest and simplest way of considering modeling errors consists of using different meshes to generate the fictitious experimental data and estimate the unknown parameters.

As shown by some plots in the previous Section, the development of damage mechanisms can be detected by estimating average stiffness parameters, whose values tend to reflect the current conditions of a structural system. Indeed, in the presence of modeling errors, it does happen that the estimates of the parameters (in general) are not accurate. However, on the basis of our results, it can be claimed that useful information is provided about the regions, which are likely to be affected by damage and might deserve special attention. In other words, the estimated values can be quite different from the actual values of the parameters, but significant changes (due to damage processes) can be clearly detected.

Apart from the modeling errors that inevitably occur when a numerical analysis is carried out with a limited number of degrees of freedom, we made an effort to simulate realistic testing conditions. To this purpose, we also assumed that we did not exactly know the zones, which were affected by damage (i.e., the zones where the stiffness parameters had actually changed and needed to be estimated).

This is a key problem of practical interest and we put some emphasis on testing conditions in which the critical zones, affected by damage, were not well defined.

If we need to cope with this problem, we might consider different mathematical models, which would provide different sets of results. In principle, however, any mesh can be reasonably accurate or basically wrong. Therefore, we tried to introduce a convenient tool with the aim of defining a level of confidence for each estimate in an objective way. The underlying idea was that a high confidence level should correspond to a reasonably accurate model of the structural system.

Thus, we introduced an error indicator, which can give a clue about the quality of the mathematical model. Essentially, it provides a measure of the estimate accuracy through a comparison between some experimental records and the corresponding structural response computed by using the parameters provided by the system identification process.

To the best of our knowledge, the error indicators defined in eqns. (6) and (7) have been used for the first time in the area of numerical simulations of non-destructive inspections,

even though the parameter  $\xi$ , determined through eqn. (6), falls in the classical context of least-squares methods. Consequently, similar applications can be found in different fields of science (cf., e.g., Abdulsadda et al. [32]). In any case, as pointed out in the previous Section, the dimensional parameter ( $\xi^*$ ), given by eqn. (7), appears to be more reliable, since it is not affected by numerical errors when the measured and/or computed quantities are much lower than their highest values and approach zero. Some results were reported in order to show that  $\xi^*$  actually represents a convenient, objective measure of the performance of a given numerical model.

As shown by the results we obtained through our simulations, the approach discussed in the paper appears to be a valuable instrument to assess the accuracy of parameter estimates, whenever system identification methods are applied. The technique is easy to implement, because it simply requires some accelerometers in order to collect adequate experimental records.

It is also suggested that the numerical model can be adjusted and improved through the information provided by a convenient error indicator. In fact, the discrepancy between a measured record and the computed response tends to decrease when the mesh is more accurate. In other words, the error indicator gets lower when a zone characterized by unknown parameters tends to coincide with a zone, which is actually subjected to a damage process.

Therefore, it appears that the present paper has focused on a non-traditional approach that is suitable to assess the development of damage processes by means of periodic non-destructive investigations. In this context, we also introduced a simple error indicator, which can provide objective information about different mathematical models, when we need to find out which one is best suited to describe the structural behavior and predict the system response.

It can be objected that this work completely ignores the complexity of dam structures and assumes the entire dam as a system that consists of macroscopically homogeneous materials characterized by elastic properties. However, as pointed out in a previous Section, nonlinear effects (e.g., at joints) would not significantly change the sensitivity of the measured quantities to ongoing damage processes.

In addition, we have focused on numerical simulations. Therefore, if we took into account the nonlinear behavior of joints, their effects should be considered both when we generate fictitious measurements and when we estimate the unknown parameters. In the end, we would have a marginal contribution to the difference between the response of the undamaged structure and its response in the presence of damage.

In general, when we consider deterioration processes which are related to the average elastic properties, any unexpected event that implies a loss of stiffness would affect the structural response, regardless of the way the surrounding structure is modeled. Nonetheless, it is clear

that joints (as well as any other significant source of nonlinearities) should be considered in the case of field tests on real structures.

In principle, nonlinearities should also be included in the numerical model when we intend to consider local effects of damage processes, such as cracks and voids. However, it seems to be practically impossible to determine the location and extension of possible cracking phenomena on the basis of some measurements, even though nowadays we can easily measure an impressive number of data (e.g., by means of radar systems). Therefore, the idea of considering the elastic properties of macroscopically homogeneous zones seems to be an acceptable compromise.

Finally, we would like to address another issue, which might raise doubts and concerns. In fact, it can be observed that the proposed procedure has not been applied, yet, to real dams monitored in the field. No doubt, in-situ tests are a fundamental requirement before we can draw any final conclusion about a monitoring technique. However, it is not so obvious to obtain, use and publicly discuss experimental results concerned with dams. Perhaps more importantly, we can hardly expect that experimental records are available, which would allow us to estimate the change of stiffness parameters in some selected areas.

Indeed, convenient long-term tests (possibly of the order of decades) would be necessary. Therefore, it appeared to be reasonable to investigate the feasibility of an experimental campaign, which could be adopted to detect possible damage processes. Clearly, this aim could only be accomplished through a numerical approach by simulating proper test conditions and including modeling errors.

---

## REFERENCES

- [1] E. Johnson, H. Lam, L. Kafatygiotis, J. Beck, Phase I IASC-ASCE Structural Health Monitoring Benchmark Problem Using Simulated Data, *J. Eng. Mech.*, Vol.130, No.1, 3-15, 2004.
- [2] J. M. W. Brownjohn, Structural health monitoring of civil infrastructure, *Phil. Trans. R. Soc. A*, Vol.365, 589-622, 2007.
- [3] U. P. Poudel, G. Fu, J. Ye, Wavelet transformation of mode shape difference function for structural damage location identification, *Earthquake Engineering and Struct. Dyn.*, Vol.36, 1089-1107, 2007.
- [4] B. Zhang, Z. Zhou, X. Li, A Crack Monitoring Method For Concrete Structures, *Intelligent Automation & Soft Computing*, Vol.16, No.5, 763-770, 2010.
- [5] I. Takewaki, M. Nakamura, S. Yoshitomi, *System Identification for Structural Health Monitoring*, WIT Press, Southampton, UK, 2012.
- [6] S. Im, S. Hurlbaas, Y. Kang, Summary Review of GPS Technology for Structural Health Monitoring, *J. Struct. Eng.*, Vol.139, 1653-1664, 2013.

- [7] A. Ohsumi, T. Kimura, M. Kono, Kalman filter-based identification of unknown exogenous input of stochastic linear systems via pseudomeasurement approach, *International Journal of Innovative Computing, Information and Control*, Vol.5, No.1, 1-16, 2009.
- [8] M. Majji, J. N. Juang, J. L. Junkins, Observer/Kalman-Filter time-varying system identification, *Journal of Guidance, Control, and Dynamics*, Vol.33, No.3, 887-900, 2010.
- [9] E. Lourens, E. Reynders, G. De Roeck, G. Degrande, G. Lombaert, An augmented Kalman filter for force identification in structural dynamics, *Mechanical Systems and Signal Processing*, Vol.27, 446-460, 2012.
- [10] Z.P. Bazant, P. C. Prat, Microplane model for brittle-plastic material: I. Theory, *ASCE Journal of Engineering Mechanics*, Vol.114, No.10, 1672-1688, 1988.
- [11] I. Carol, E. Rizzi, K. Willam, An 'extended' volumetric/deviatoric formulation of anisotropic damage based on a pseudo-log rate, *European Journal of Mechanics A/Solids*, Vol.21, 747-772, 2002.
- [12] H. Park, J. Kim, Plasticity model using multiple failure criteria for concrete in compression, *International Journal of Solids and Structures*, Vol.42, 2303-2322, 2005.
- [13] C. H. Loh, T. S. Wu, Identification of Fei-Tsui arch dam from both ambient and seismic response data, *Soil Dynamics and Earthquake Engineering*, Vol.15, 465-483, 1996.
- [14] K. W. Hudnut, J. A. Behr, Continuous GPS monitoring of Structural Deformation at Pacoima Dam, California, *Seismological Research Letters*, Vol.69, No.4, 299-308, 1998.
- [15] M. Stewart, M. Tsakiri, The Application of GPS to Dam Surface Monitoring, *Journal of Geospatial Engineering*, Vol.3, No.1, 45-57, 2001.
- [16] G. R. Darbre, J. Proulx, Continuous ambient-vibration monitoring of the arch dam of Mauvoisin, *Earthquake Engng and Struct. Dyn.*, Vol.31, 475-480, 2002.
- [17] R. Fedele, G. Maier, B. Miller, Identification of elastic stiffness and local stresses in concrete dams by in situ tests and neural networks, *Structure and Infrastructure Engineering*, Vol.1, No.3, 165-80, 2005.
- [18] C. Jin, M. Soltani, X. An, Experimental and numerical study of cracking behaviour of openings in concrete dams, *Computers and Structures*, Vol.83, 525-535, 2005.
- [19] A. De Sortis, P. Paoliani, Statistical analysis and structural identification in concrete dam monitoring, *Engineering Structures*, Vol.29, 110-120, 2007.
- [20] M. Alba, G. Bernardini, A. Giussani, P. P. Ricci, F. Roncoroni, M. Scaioni, P. Valgoi, K. Zhang, Measurement of dam deformations by terrestrial interferometric techniques, *The International Archives of the Photogrammetry, Remote Sensing and Spatial Information Sciences*, Vol.37, B1, 133-139, 2008.
- [21] J. Boavida, A. Oliveira, A. Berberan, Dam monitoring using combined terrestrial imaging systems, *Proc. 4th IAG Symposium on Geodesy for Geotechnical and Structural Engineering*, Lisbon, Portugal, 475-480, 2008.
- [22] R. E. Kalman, A new approach to linear filtering and prediction problems, *Trans. ASME, J. Basic Engng.*, Vol.82, 35-45, 1960.
- [23] P. Eikhoff, *System Identification*, John Wiley, Chichester, UK, 1983.
- [24] A. Nappi, G. Facchin, Monitoring of Damaged Zones in Large Dams: An Error Indicator to Evaluate a Non-Destructive Testing Procedure, *AES Technical Reviews Journals*, Vol.4, 11-21, 2011.
- [25] International Commission on Large Dams (ICOLD), 6th International Benchmark Workshop on Numerical Analysis of Dams, Theme A – Concrete dams, 2001.
- [26] A. Nappi, G. Facchin, Damage assessment in dams: a Kalman Filter approach, *AES Technical Reviews International Journal*, Vol.1, No.1, 45-53, 2008.
- [27] C. Hu, W. Chen, Y. Chen, D. Liu, Adaptive Kalman Filtering for Vehicle Navigation, *Journal of Global Positioning Systems*, Vol.2, No.1, 42-47, 2003.
- [28] D.J. Jwo, S.H. Wang, Adaptive fuzzy strong tracking extended Kalman filtering for GPS navigation, *IEEE Sensors Journal*, Vol.7, No.5, 778-789, May 2007
- [29] F. Lenartz, C. Raick, K. Soetaert, M. Grégoire, Application of an ensemble Kalman filter to a 1-D coupled hydrodynamic-ecosystem model of the Ligurian Sea, *Journal of Marine Systems*, Vol.68, 327-348, 2007
- [30] C. Antoniou, A. Kondyli, G.M. Lykogianni, E. Gyftodimos, Exploratory assessment of the limiting Extended Kalman Filter properties, *Transport and Telecommunication Journal*, Vol.14, No.1, 1-12, March 2013
- [31] J. Fossier, D. Teichmann, J. Jia, B. Misgeld, S. Leonhardt, An adaptive Kalman filter approach for cardiorespiratory signal extraction and fusion of non-contacting sensors, *BMC Medical Informatics and Decision Making*, 14:37, 2014
- [32] A. Abdulsadda, N. Bouaynaya, K. Iqbal, Stability Analysis and Breast Tumor Classification from 2D ARMA Models of Ultrasound Images, *IEEE International Conference of the Engineering in Medicine and Biology Society (EMBC'09)*, Minneapolis, MN, September 2009